Electronic Supplementary Material (ESI) for ChemComm.

Design of Phase-Transition Molecular Solar Thermal Energy Storage Compounds: Compact Molecules with High Energy Densities

Qianfeng Qiu, Mihael A. Gerkman, Yuran Shi, and Grace G. D. Han*

Department of Chemistry, Brandeis University, 415 South Street, Waltham, MA 02453, USA

Email: gracehan@brandeis.edu

Table of Contents

1. General Methods

All reactions were monitored by thin-layer chromatography (TLC) using Merck silica gel 60 F254 plates (0.25 mm). TLC plates were visualized using UV light (254 nm). Silica column chromatography was performed using Merck Silica Gel 60 (230–400 mesh). ^{1}H NMR were recorded on a Bruker Avance 400 spectrometer at 400 MHz.

UV-Vis Absorbance Spectroscopy:

UV−Vis adsorption spectra of compounds **1**-**2** and **4**-**9** were obtained with a Cary 50 Bio UV−vis spectrophotometer in a UV Quartz cuvette with a path length of 10 mm. Compounds were dissolved in chloroform at a concentration of 0.0125 mg/ml. The UV−vis absorption was first recorded in dark for 3-5 min, then samples were irradiated with a specified wavelength until no change in their absorbance was observed. Samples were irradiated with a series of Thorlabs LEDs: M365LP1 (365 nm, 21.0 μW/mm^2, 2000 mW), M340L4 (340 nm, 2.22 μW/mm^2, 60 mW), M395L4 (395 nm, 6.7 μW/mm^2, 535 mW), M430L4 (430 nm, 35.3 μW/mm^2, 600 mW), M530L3 (530 nm 9.5 μW/mm^2, 370 mW), M565L3 (565 nm, 11.7 μW/mm^2, 979 mW), and M590L3 (590 nm, 5.3 μW/mm^2, 170 mW). The UV-vis spectra of compound **3** were reported.[1] The condensed-state UV-vis adsorption spectra of compounds **1**-**9** were collected with the same spectrophotometer using ultra-thin films (0.7-1.2 μm thick).

Differential Scanning Calorimetry (DSC):

DSC analysis was conducted on a DSC 250 (TA Instruments) with an RSC 90 cooling component. All samples were heated at a rate of 10 °C/min unless otherwise noted. All *E* isomers were melted and cooled to −90 °C before reheating. Liquid *Z* isomers of compounds **1**, **2**, and **6**-**8** were first cooled to −90 °C then heated. Solid *Z* isomers of compounds **3**-**5** and **9** were melted and cooled to −90 °C. In DSC experiments with a scan rate of 10 °C/min (unless otherwise specified), the *Z* isomers were heated below their respective T_{iso} to prevent the *Z*-to-*E* thermal reversion. To determine the ΔH_{iso} of *Z* isomers, samples were heated from 20 °C until the thermal isomerization was completed.

Preparation of *Z*-isomer Samples for DSC Measurement:

Z isomers were obtained by dissolving each *E* isomers in dichloromethane and irradiating the sample with an appropriate wavelength of light until a photostationary state was reached. *Z*-rich samples were concentrated, dried under high-vacuum, and then transferred to DSC pans for analysis. Compounds **3** and **5** were further purified by chromatography to get a higher ratio of *Z* isomers before DSC measurement.

Thin Film Preparation:

Thin-film samples were prepared by adding 0.1 mL of 12.5 mg/mL DCM solution of *E* isomers on a clean glass slide (1.2 x 1.2 cm^2) and heating it on a hot plate until the solvent was totally evaporated, leaving a molten sample. The melt was covered by another glass slide to spread and fill the entire area of glass substrate. Then the sample was slowly cooled to room temperature. Temperature was controlled using a VWR Advanced hot plate stirrer.

Photo-isomerizing thin film samples of compounds **3** and **6** was performed by the following procedure. A thin film was heated in dark above the T_m of *E* isomer. Then the sample was cooled to 10 °C above the T_c of *E* isomer and irradiated with 340 nm LED for 1 h and gradually cooled down to room temperature under continuous UV irradiation for another 1 h to reach the PSS of *E*-*Z* photoisomerization. *E*-*Z* photoisomerization of thin film samples of compounds **1** and **2** were achieved by the direct irradiation with 365 nm light for 2 h at room temperature.

Optical crystallization of liquid phase films of compounds **1** and **2** was performed by irradiating the samples by 430 nm LED for 5 to 60 min at room temperature.

Digital images of thin films were taken on a microscope Olympus SZ-CTV by camera Olympus Q-Color3 at room temperature.

The ultra-thin films of *Z* isomers were prepared by adding 0.1 mL of 5 mg/mL DCM solution of compounds **1-9**, which had been irradiated under 340 nm or 365 nm overnight, on a clean glass slide (2.5 x 2.5 cm^2). Solvent was evaporated at room temperature in dark, leaving a liquid material. The liquid was covered by another glass slide to spread and fill the entire area of glass substrate. Then the liquid-state ultra-thin films of *Z* isomers were characterized by UV-vis spectroscopy. The ultra-thin films of *Z* isomers were cooled down in a fridge to crystallize, and the solid films were characterized by UV-vis spectroscopy. Then the films were heated to isomerize to *E* isomers in liquid state, which was characterized by UV-vis spectroscopy. Upon cooling to room temperature, the crystallized solid *E* isomers were characterized by UV-vis spectroscopy again.

Bulk Sample *E*-*Z* Isomerization:

The bulk sample isomerization was conducted with 200 mg of crystalline compound **2** contained in a UV quartz cuvette with a pathlength of 10 mm. The cuvette was placed on a piece of black paper and a stir plate (600 rpm) under 365 nm LED at room temperature for 12 h. Then the liquid sample was irradiated with 590 nm LED under the identical condition for 12 h. Digital photos were taken by Cannon EOS REBEL SL2 200D. The ratios of *Z* isomer in the sample were determined by ^{1}H NMR.

Theoretical Calculations:

Compounds **1**-**4**, **8**, and **9** were optimized to their minimum-energy geometry by using the Density Functional Theory (DFT) framework at the RB3LYP/6-31G(d,p) level of theory.[2,3] Compounds **5**-**7** were optimized by using RB3LYP/6-LAN2DZ.[4,5] Among all the possible conformations for both *E* and *Z* isomers, the most stable structures were chosen to analyze the magnitude of the molecular dipole moment. All calculations were performed by using the Gaussian 09W suite of programs.

2. Synthesis of azobenzene derivatives

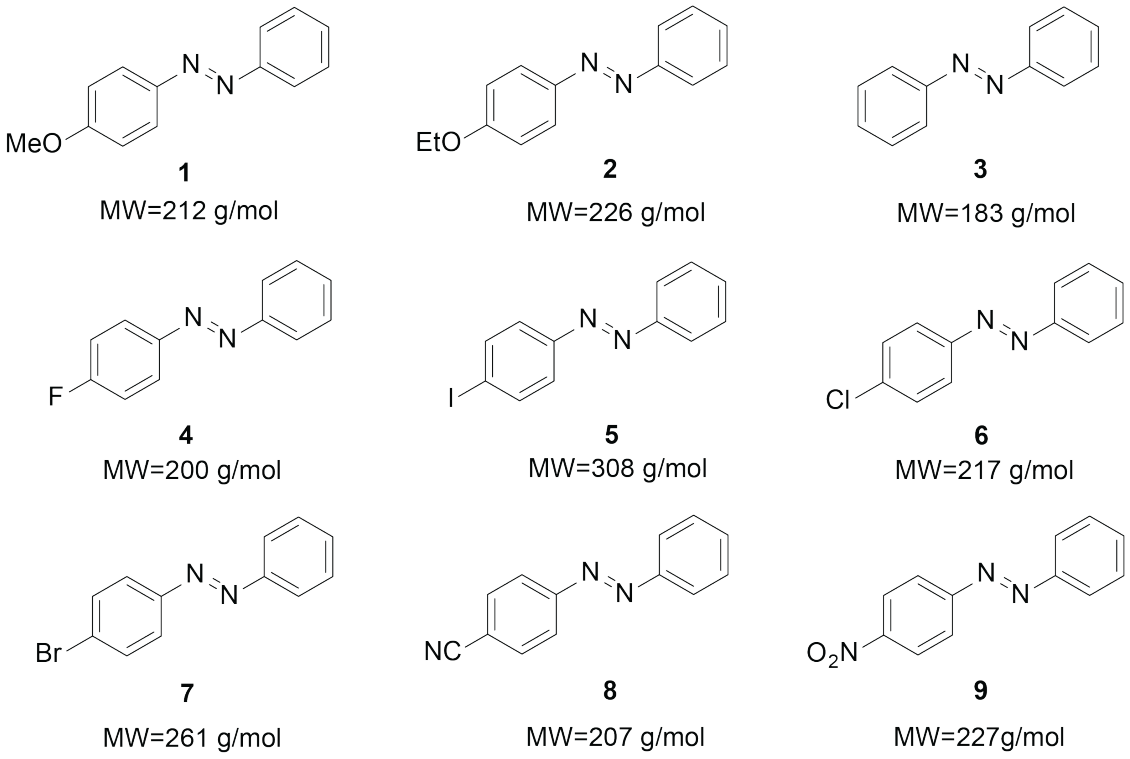

Scheme 1. Structures of compounds **1-9**.

Compounds **1** and **3** were purchased from Sigma-Aldrich, without further purification. Compounds **2** and **4-9** were prepared according to the previous literature procedures as follows.[6–9]

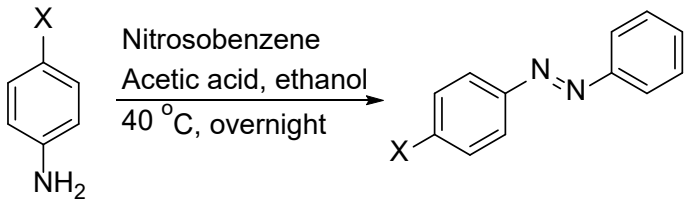

To a solution of nitrosobenzene (0.5 g, 4.7 mmol) in glacial acetic acid (12 mL) and EtOH (3 mL), the corresponding amine (1.0 equiv) was added. The reaction mixture was stirred at 40 °C overnight. Then, the mixture was diluted by 50 mL DCM and further neutralized by 5% $NaHCO_3$ solution. The two-layer mixture was extracted with 50 mL DCM for 3 times. The organic layer was collected, washed with brine, dried over anhydrous $MgSO_4$, and concentrated on a rotary evaporator. The crude product was further purified with silica gel chromatography (hexane and ethyl acetate mixture). All products were isolated as orange solids (yields: compound **2** = 62%, compound **4** = 65%, compound **5** = 54%, compound **6** = 67%, compound **7** = 71%, compound **8** = 34%, compound **9** = 31%). ^{1}H NMR spectra matched reported values.

3. Computational results

Table S1. Summary of dipole moment of *E* and *Z* isomers of compounds **1-9**.

Compound	1	2	3	4	5	6	7	8	9
Dipole of *E* *(Debye)*	1.88	1.65	0.00	1.28	1.89	2.65	2.31	5.55	5.93
Dipole of *Z* *(Debye)*	4.50	4.08	3.20	2.41	3.08	2.92	2.97	3.88	4.20

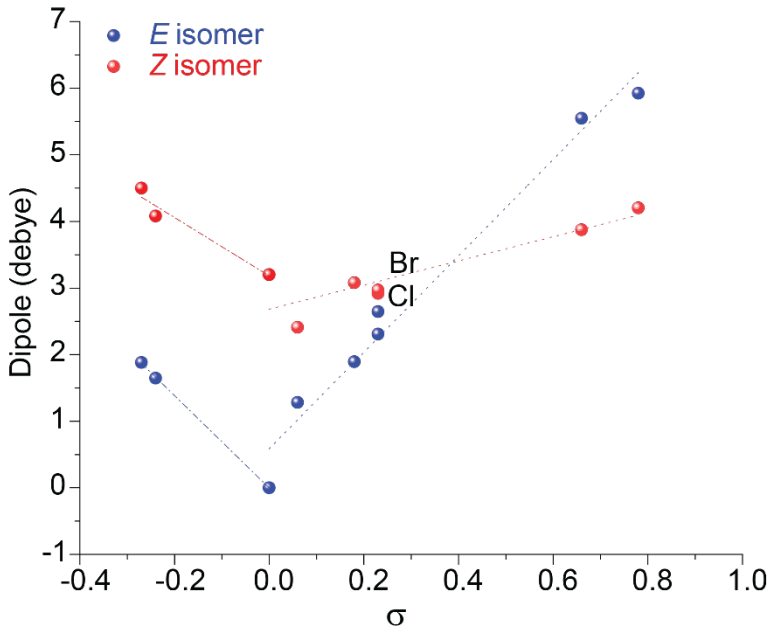

Fig. S1. Correlation between Hammett constants and dipole moments of *E* and *Z* isomers of compounds **1-9**.

4. Photoswitching properties

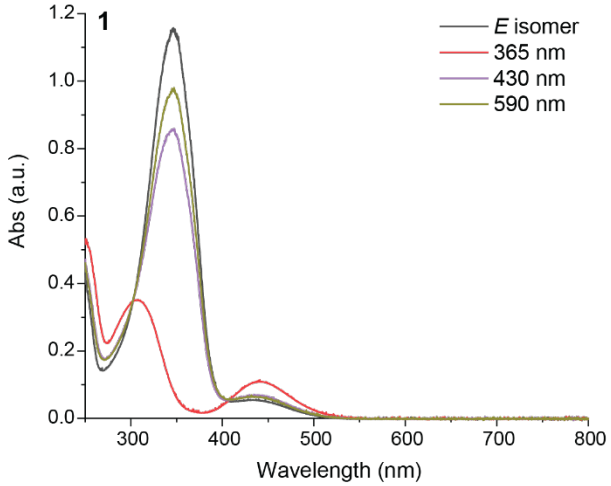

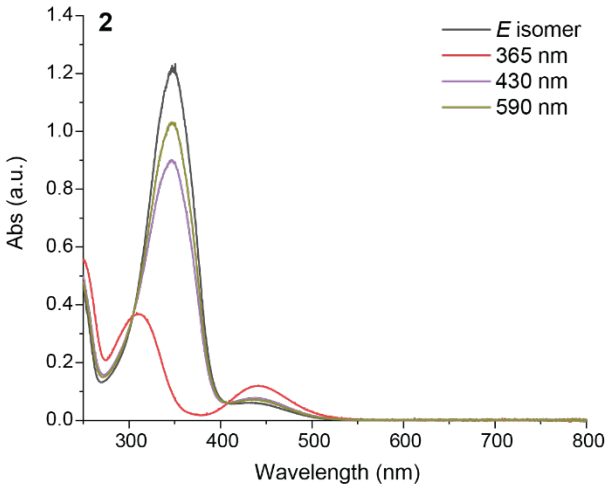

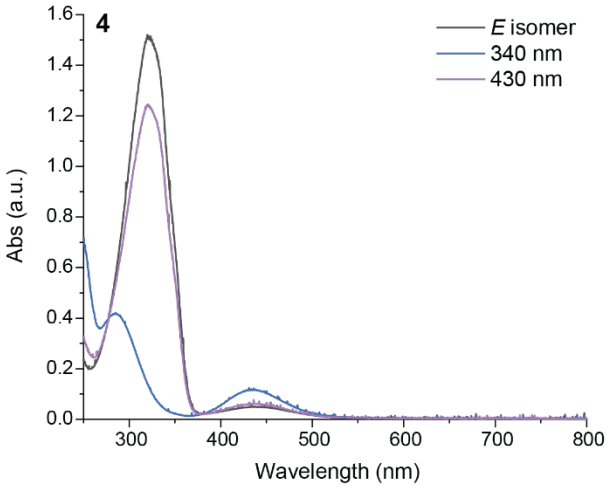

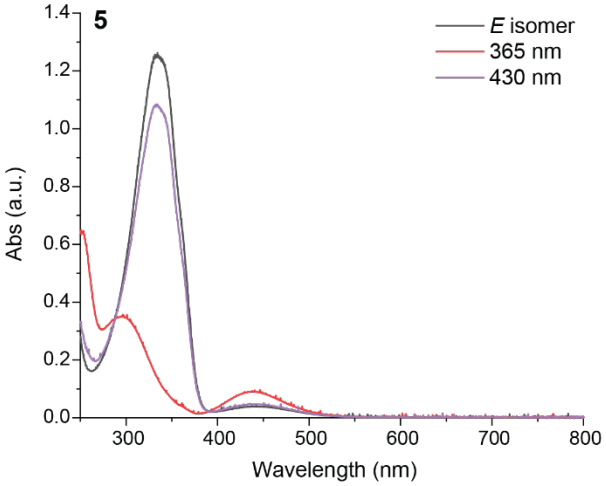

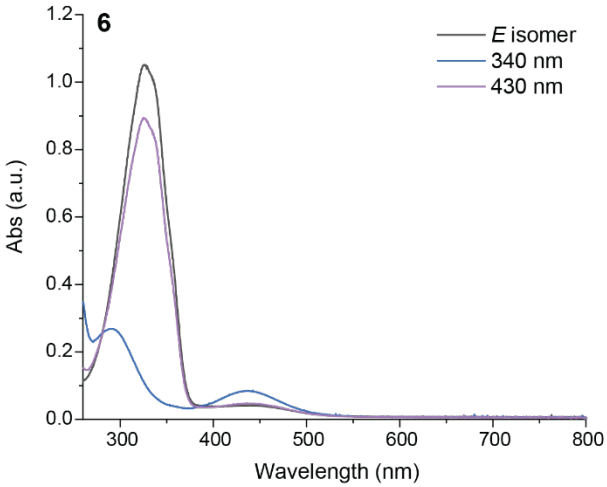

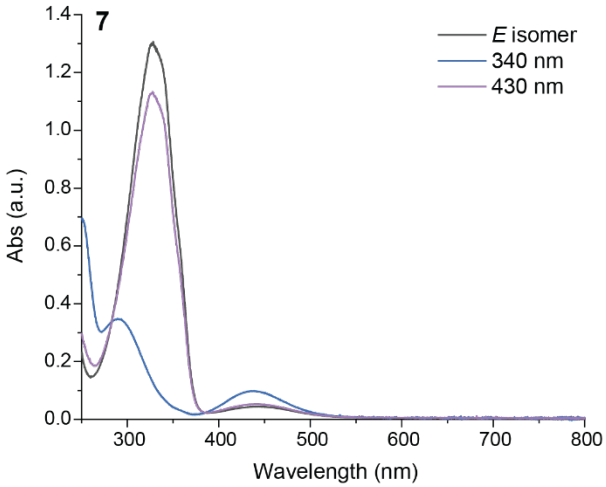

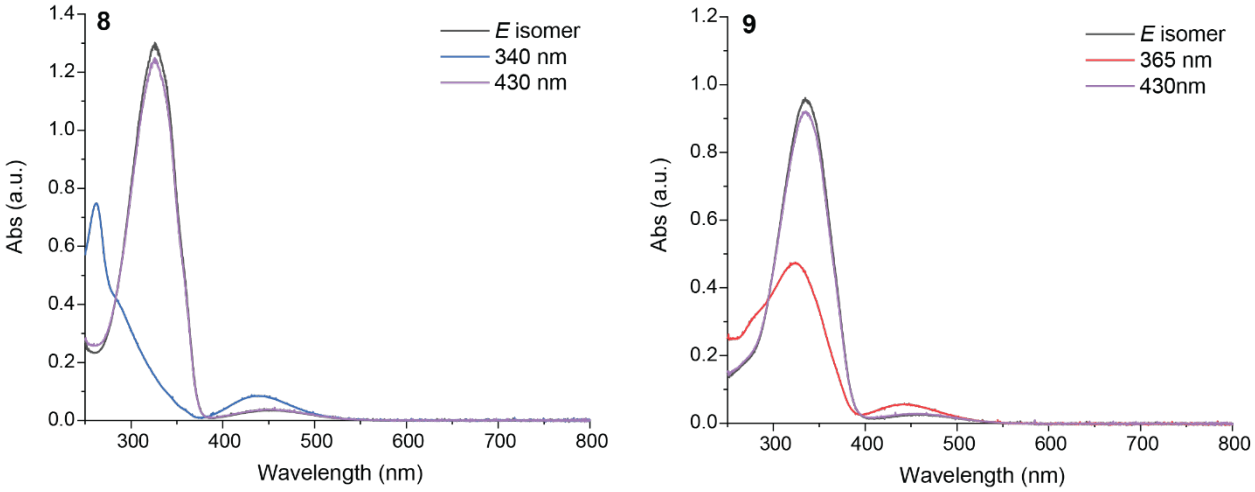

Fig. S2. UV-Vis absorption spectra of compounds **1**-**2** and **4**-**9** in chloroform solutions.

Table S2. Percentage (%) of *Z* isomers in UV-irradiated solution samples and condensed films ([a] irradiated by 365 nm, [b] irradiated by 340 nm). [*]Due to the suboptimal %*Z* achieved in solution, further column chromatography purification of *Z* isomer was performed to maximize %*Z* and clearly determine the optical and thermal parameters reported in Fig. S2-S3 and Table S3-S5). \: The compounds exhibit melting points greater than their thermal isomerization temperatures, so the condensed phase charging was not viable.

	Compound	**1**	**2**	**3**	**4**	**5**	**6**	**7**	**8**	**9**
%Z	Solution	[a]96	[a]91	[b*]81	[b]98	[a*]91	[b]95	[b]94	[b]92	[a]47
	Condensed phase	[a]92	[a]80	[b]53	[b]75	\	[b]55	[b]18	\	\

- %*Z* measurement for solution state: *E* isomers were dissolved in dichloromethane and irradiated with an LED until a photostationary state was reached. *Z*-rich samples were concentrated, dried under high-vacuum, and analyzed by ^{1}H NMR.
- %*Z* measurement for condensed phase: For compounds **3-9**, thin films prepared according to our method were heated in dark above the T_m of *E* isomer. Then the films were cooled to 10 °C above the T_c of *E* isomer and irradiated with an LED for 1 h. Films were gradually cooled down to room temperature under continuous UV irradiation for another 1 h. For compounds **1** and **2**, the films were irradiated by an LED at room temperature for 2 h. %*Z* of the irradiated films were determined by the ^{1}H NMR analysis of the dissolved films.

5. Differential scanning calorimetry plots

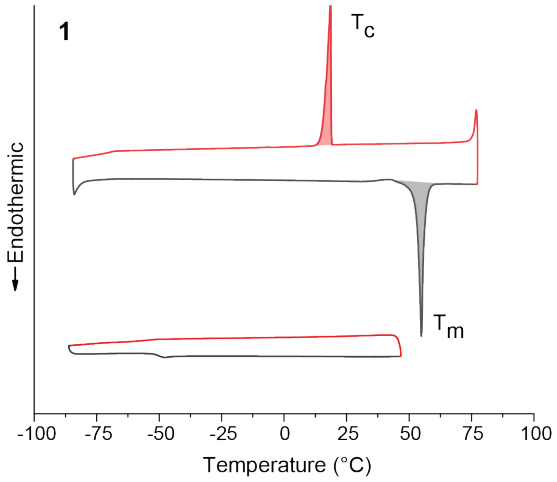

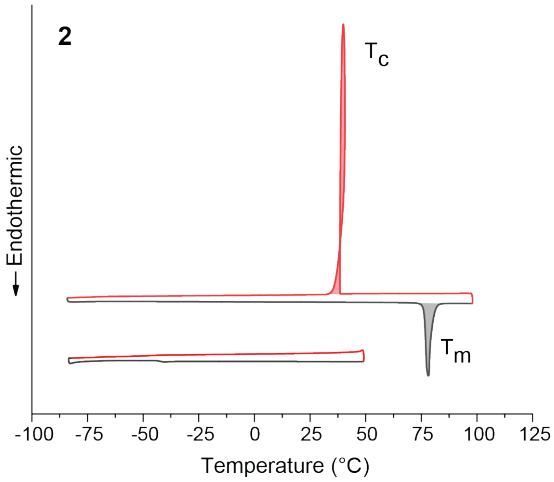

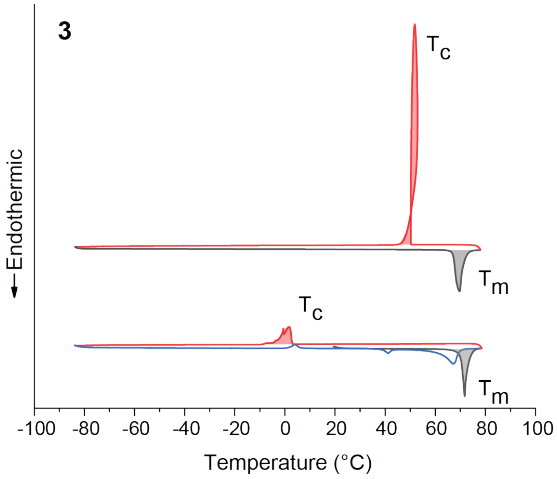

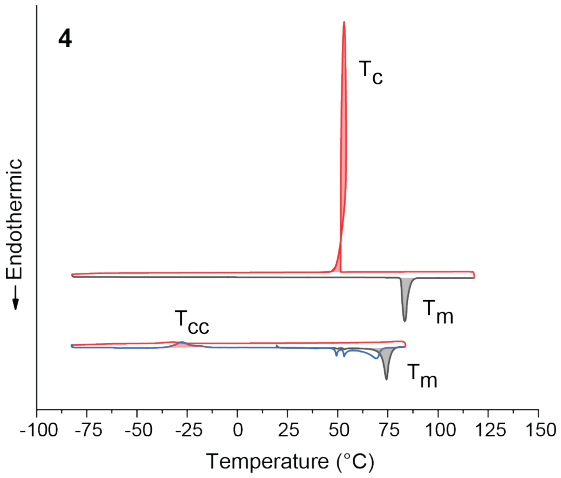

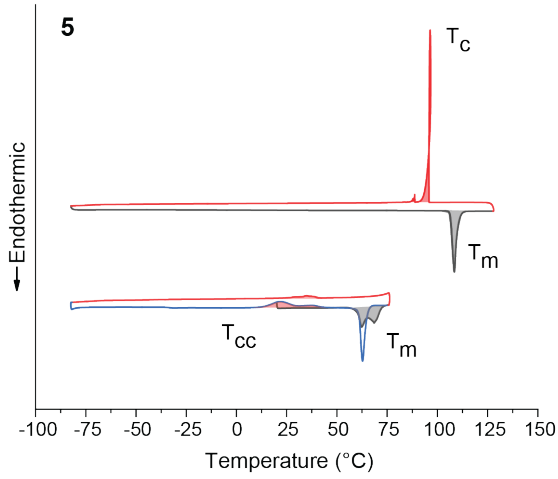

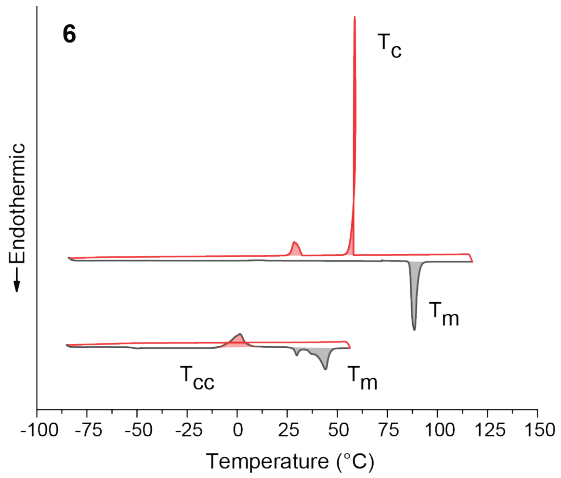

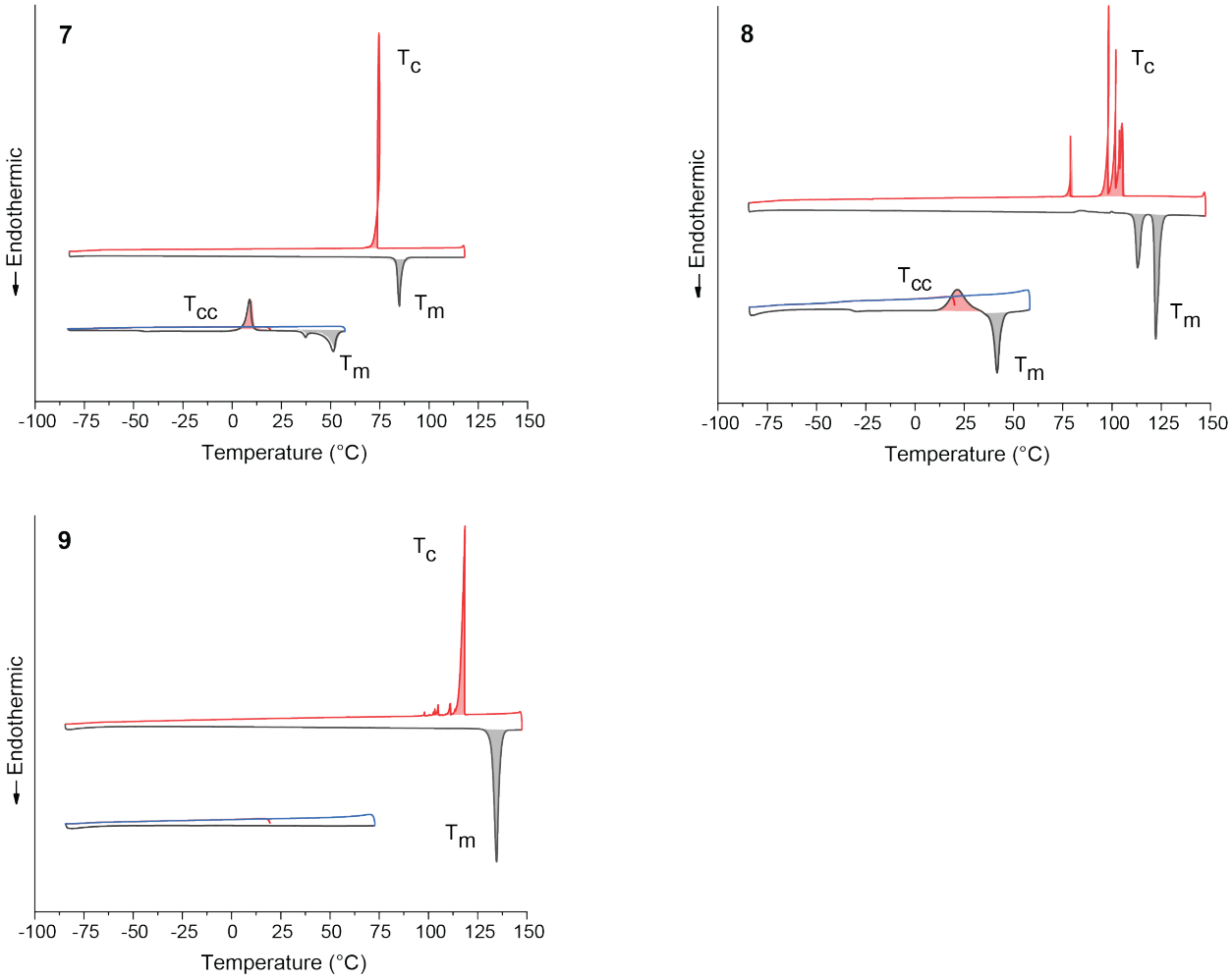

Fig. S3. DSC plots illustrating thermal properties of *E* (top curve) and *Z* (bottom curve) isomers upon heating and cooling for compounds **1-9**. The following thermal parameters are labeled in plots: crystallization temperature (T_c), melting temperature (T_m), and cold-crystallization temperature (T_{cc}). Scan rate is 10 °C/min. The first heating curve is shown in grey, first cooling in red, and second cooling or heating in blue.

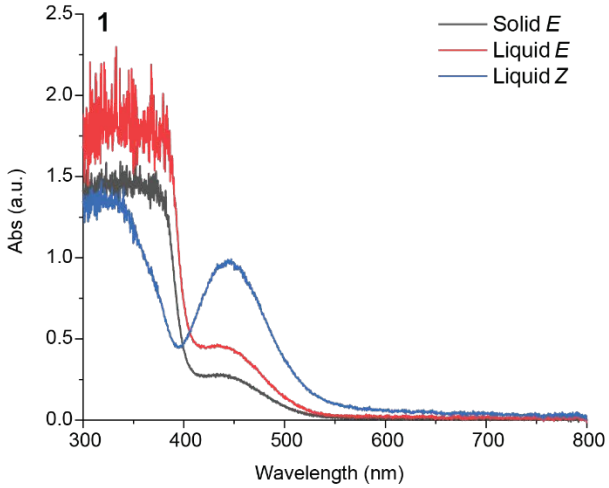
1
Solid E
Liquid E
Liquid Z
Abs (a.u.)
Wavelength (nm)

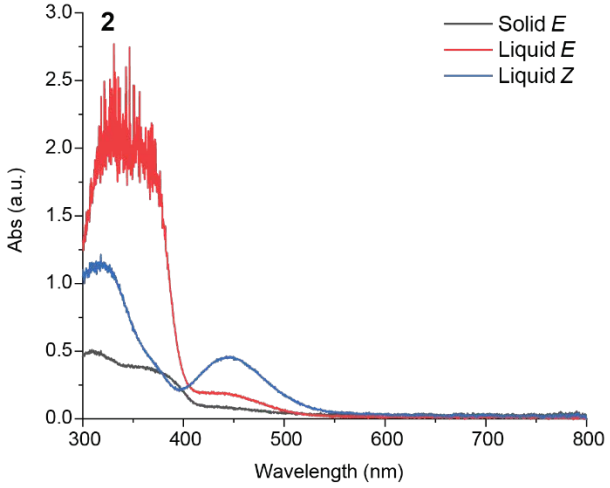
2
Solid E
Liquid E
Liquid Z
Abs (a.u.)
Wavelength (nm)

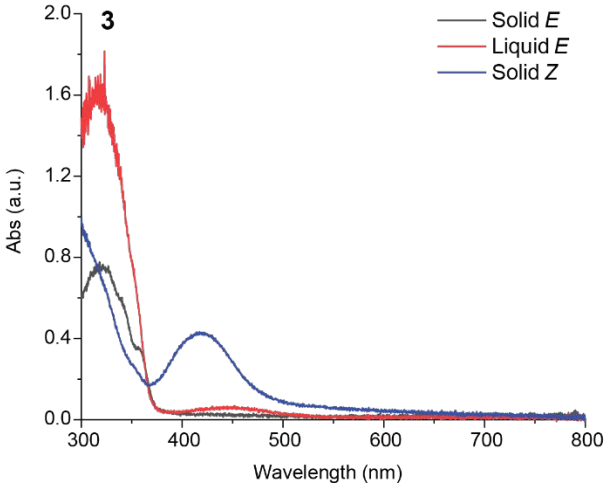
3
Solid E
Liquid E
Solid Z
Abs (a.u.)
Wavelength (nm)

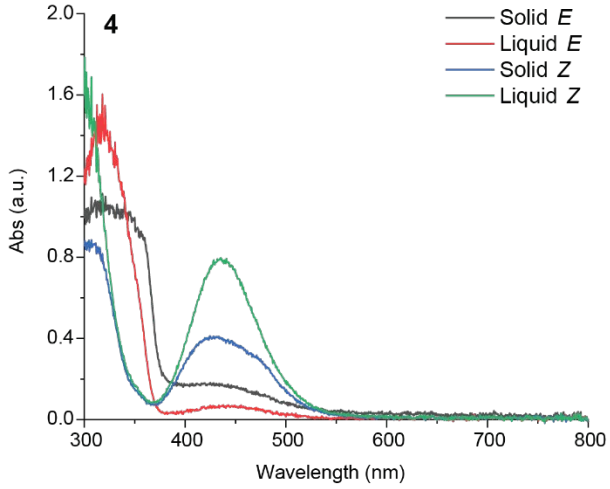
4
Solid E
Liquid E
Solid Z
Liquid Z
Abs (a.u.)
Wavelength (nm)

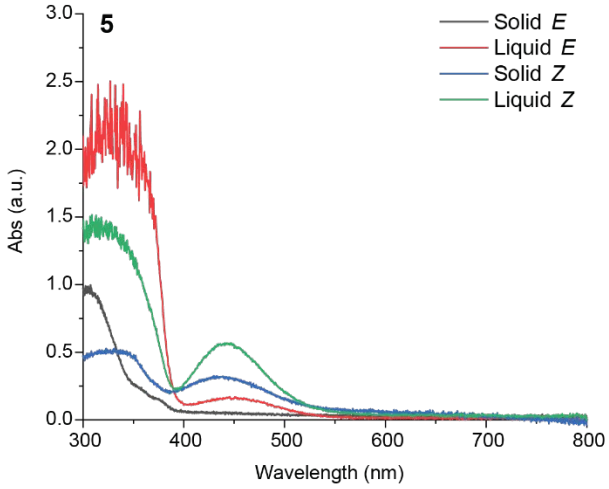
5
Solid E
Liquid E
Solid Z
Liquid Z
Abs (a.u.)
Wavelength (nm)

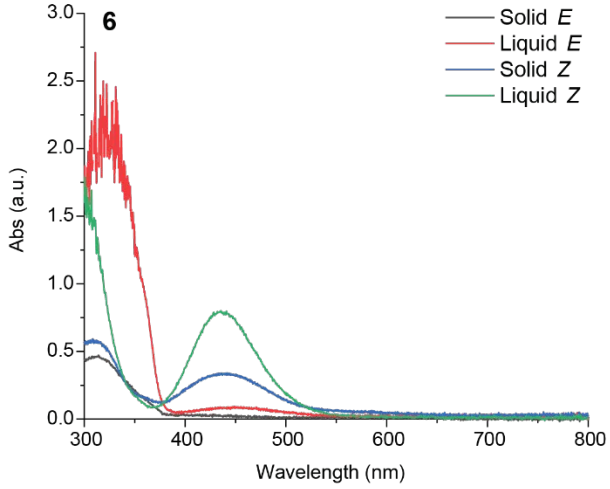
6
Solid E
Liquid E
Solid Z
Liquid Z
Abs (a.u.)
Wavelength (nm)

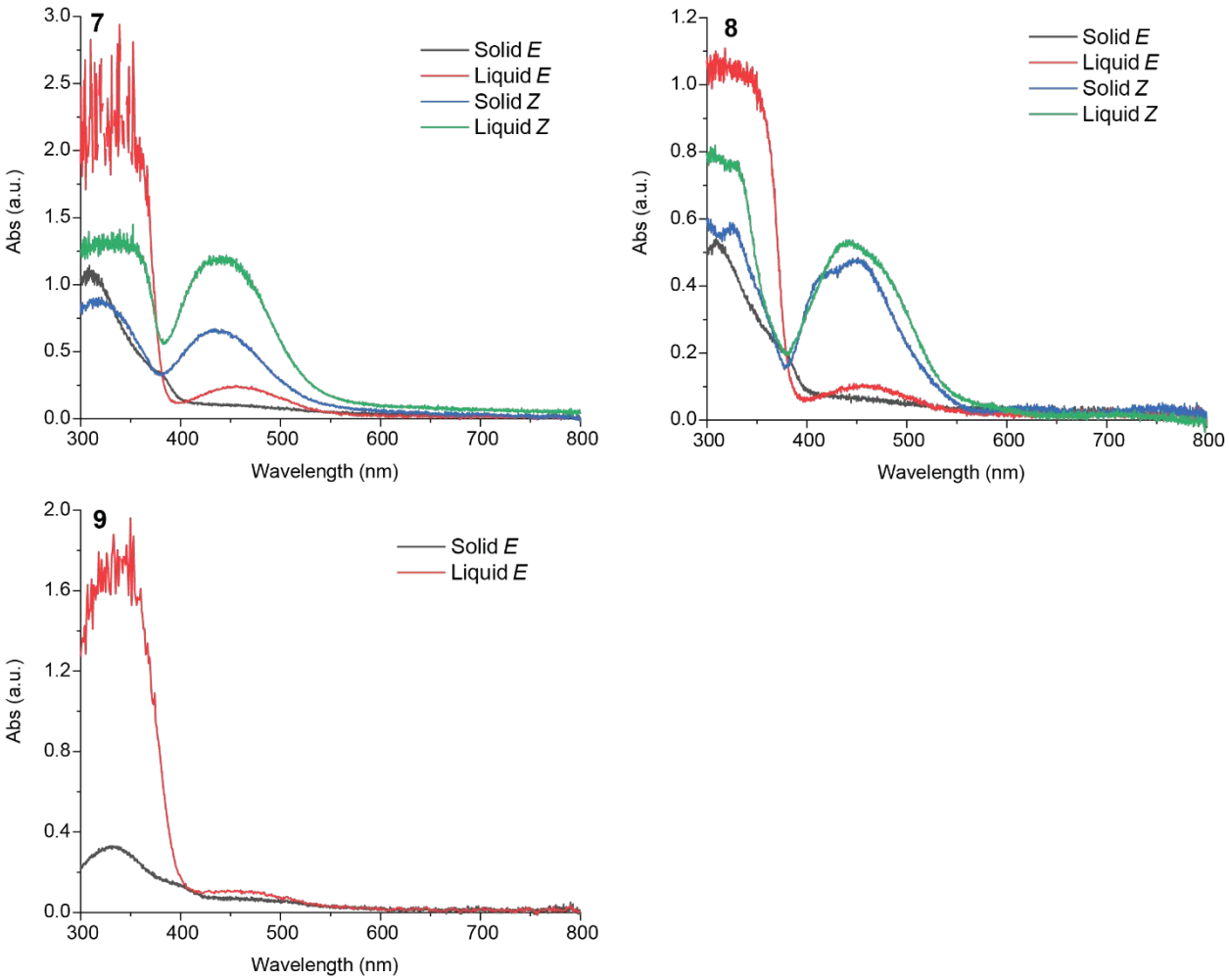

Fig. S4. UV-vis absorption spectra of compounds **1-9** in condensed phases. Compounds **1** and **2** only exhibit liquid phase as *Z* isomers that are achieved by the direct irradiation of solid *E* film at room temperature. *Z* liquid of compound **3** instantly crystallized in thin films, thus showing only *Z* solid absorption profile. A high concentration of *Z* isomer of compound **9** was difficult to achieve due to its short $t_{1/2}$. We note that *Z* isomers of compounds **3-9** have been pre-irradiated in solution and dried to form respective condensed phases. This shows the clear absorption difference between *E* and *Z* isomers in condensed phases. The PSS ratios between *E* and *Z* under UV irradiation in condensed phases are summarized in Table S2. The mixture of *E* and *Z* isomers will display intermediate absorption characteristics between *E* and *Z* spectra.

Table S3. Thermal parameters of *E* and *Z* isomers measured by DSC. Peak temperature of each thermal transition is reported. Cold-crystallization peak (cc), melting enthalpy (ΔH_m), crystallization enthalpy (ΔH_c).

	***E* isomer**				***Z* isomer**			
Compound	T_m (°C)	ΔH_m (J/g)	T_c (°C)	ΔH_c (J/g)	T_m (°C)	ΔH_m (J/g)	T_c (°C)	ΔH_c (J/g)
1	55	76	18	59	Liq	Liq	Liq	Liq
2	78	118	38	103	Liq	Liq	Liq	Liq
3	70	129	51	126	72	112	2	70
4	84	127	54	118	75	126	-32^{cc}	73^{cc}
5	108	72	96	65	62	70	35^{cc}	49^{cc}
6	89	134	59	116	45	90	2^{cc}	59^{cc}
7	85	70	74	69	52	71	10^{cc}	61^{cc}
8	122	149	106	134	42	72	22^{cc}	62^{cc}
9	135	136	119	129	Sol/Liq	Sol/Liq	Sol/Liq	Sol/Liq

Table S4. The summary of *E* isomer enthalpy of melting and crystallization, *Z*-to-*E* thermal isomerization enthalpy for 100% *Z* content, and their total energy storage during the phase transition and isomerization in kJ/mol.

Compound	**1**	**2**	**3**	**4**	**5**	**6**	**7**	**8**	**9**
***E*-ΔH_m (kJ/mol)**	16	27	23	25	22	29	18	31	31
***E*-ΔH_c (kJ/mol)**	12	23	23	24	20	25	18	28	29
ΔH_{iso} (kJ/mol)	49	56	43	42	49	49	47	43	23
ΔH_{total} (kJ/mol)	62	79	66	65	69	74	65	71	52

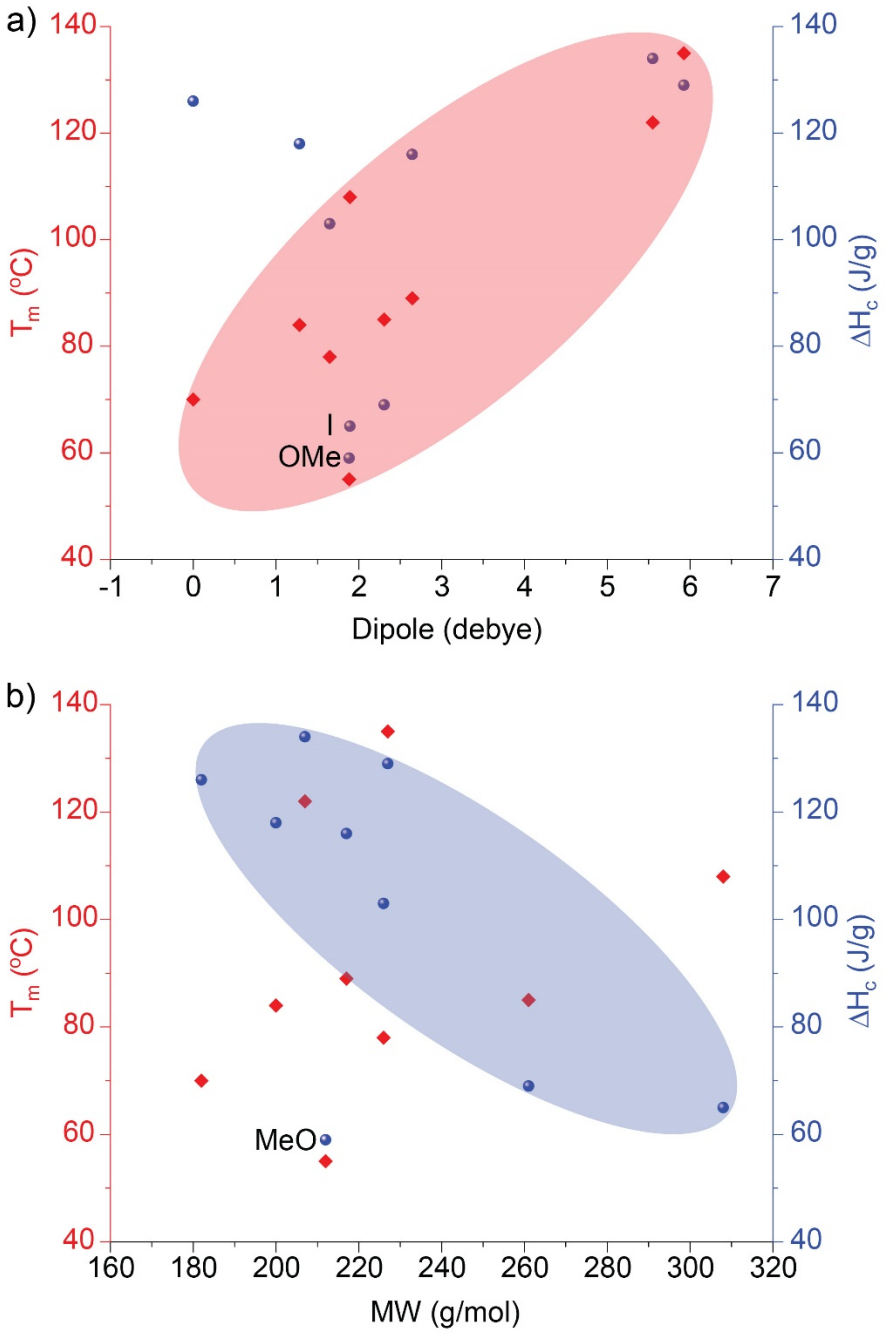

Fig. S3. Melting points and crystallization enthalpy of *E* isomers of compounds **1-9** as a function of a) DFT-calculated dipole moment of *E* and b) the molecular weight of compounds. Compound **1** shows an exceptionally low ΔH_c due to the reduced π–π interactions between aromatic cores.

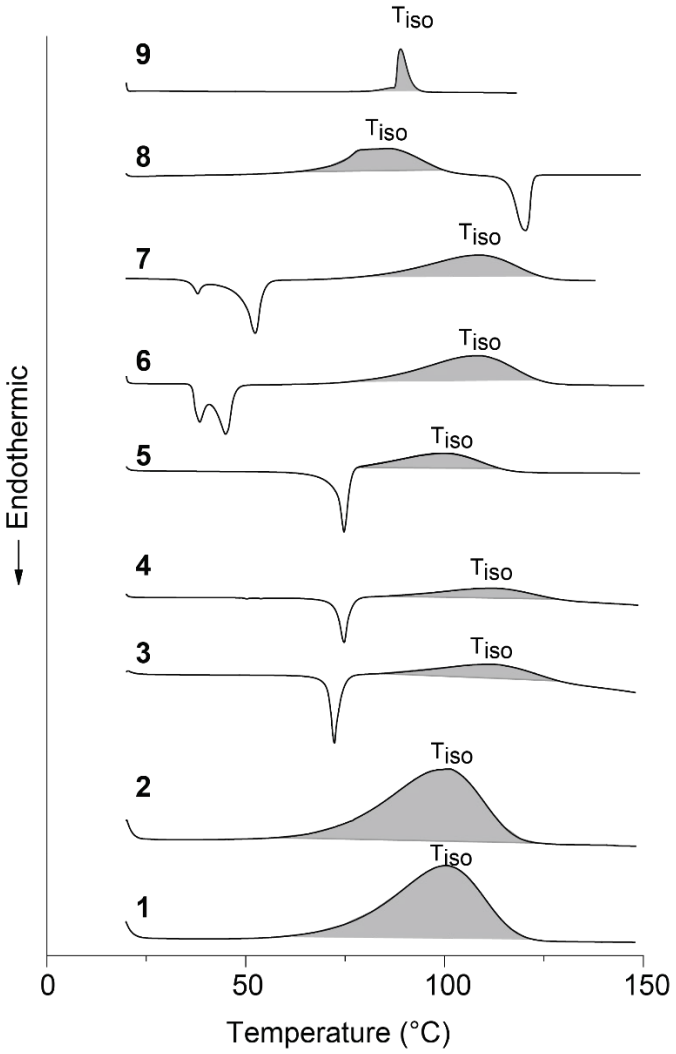

Fig. S4. DSC plots illustrating the thermal isomerization of *Z* isomers for compounds **1**-**9** showing the temperature range of thermal *Z*-to-*E* isomerization, the peak temperature (T_{iso}), and isomerization energy (integrated area under the exothermic curves, highlighted in grey). For compound **8** and **9**, the areas represent a sum of isomerization energy and crystallization energy). Scan rate is 10 °C/min for compounds **1**-**4**, **6**-**7**, and **9**, 5 °C/min for compound **5** and **8**, which was used to resolve the overlapping isomerization and melting endotherms or crystallization exotherms, respectively.

Table S2. The summary of peak thermal isomerization temperature and isomerization energy of compounds **1-9**. ([#] sum of isomerization enthalpy and *E* crystallization enthalpy; ***** calculated by deducting the *E* isomer crystallization energy from the integrated exotherm, and calibrating the isomerization enthalpy for 100% *Z* content).

Compound	**1**	**2**	**3**	**4**	**5**	**6**	**7**	**8**	**9**
Temperature (°C)	101	101	113	113	90	109	109	86	86
ΔH_{iso} (J/g)	224	224	235	204	158	216	169	[#]315	[#]108
ΔH_{iso} (J/g) *Z*%=100%	233	246	235	208	158	227	180	[*]209	[*]100

6. Thermal reversion kinetics

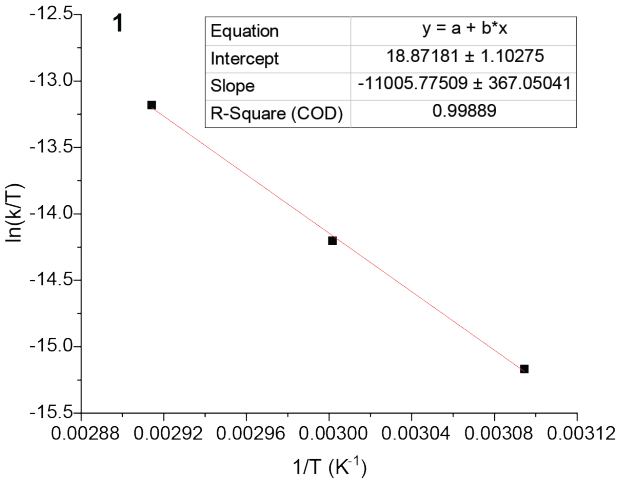

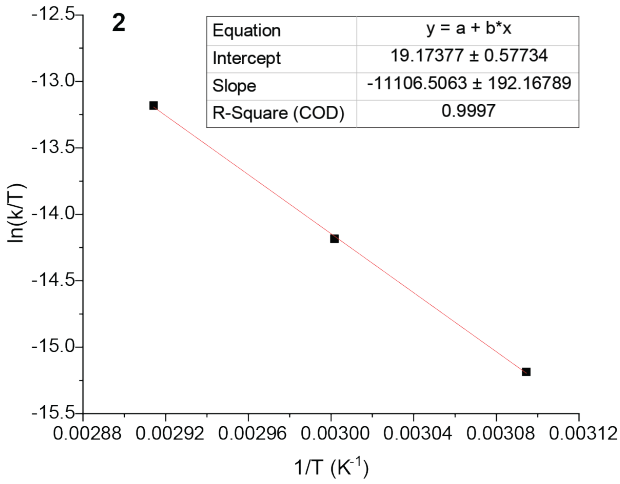

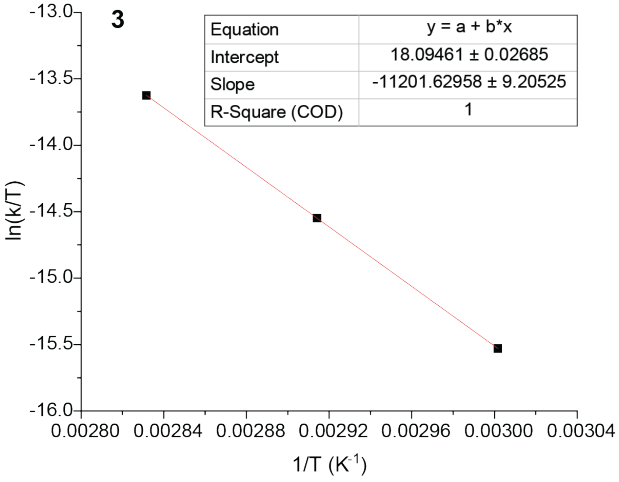

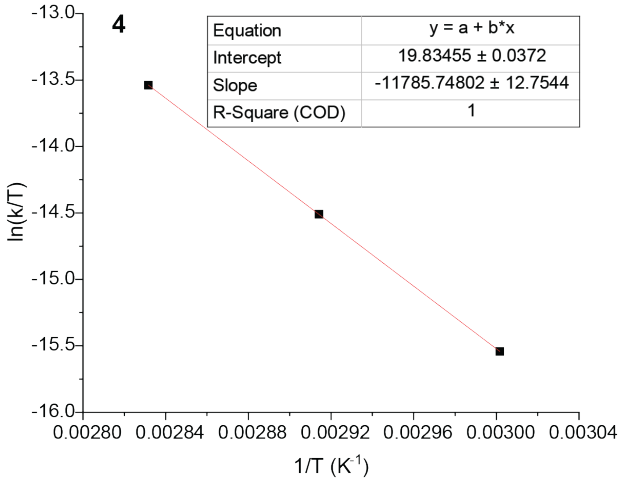

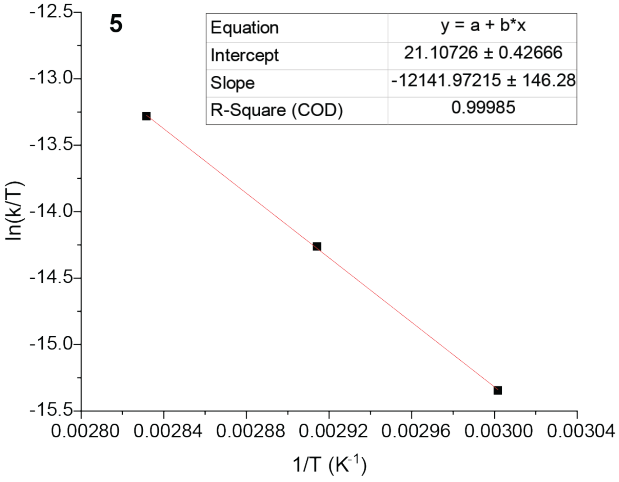

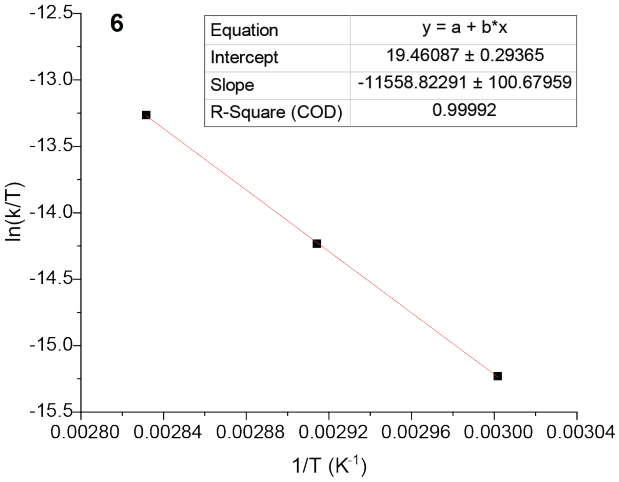

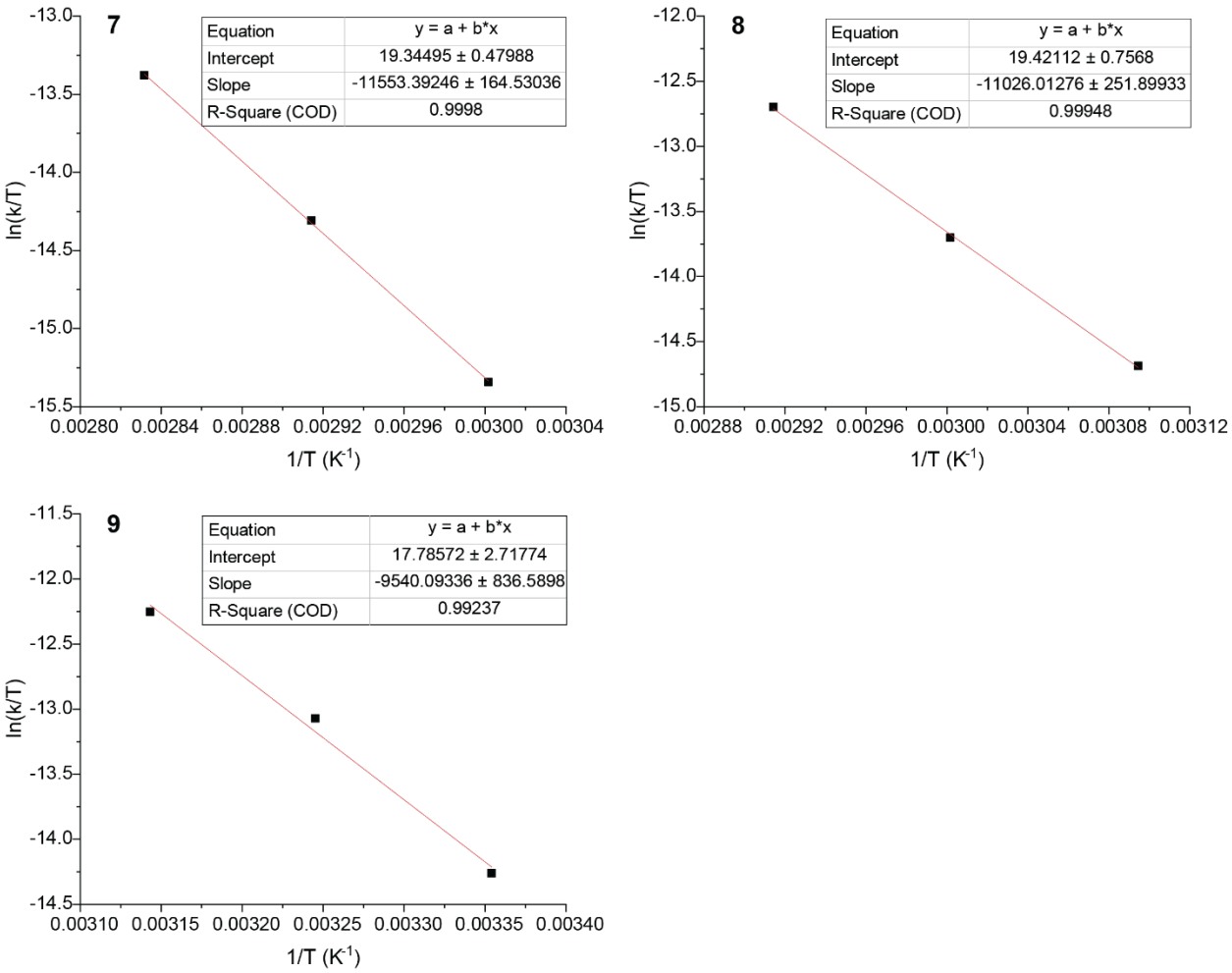

Fig. S5. Eyring-Polanyi plots of thermal Z-to-E isomerization of compounds **1-9** measured in DMSO.

Table S3. Summary of thermal reversion activation energy ($\Delta H^{\ddagger}$, $\Delta S^{\ddagger}$, $\Delta G^{\ddagger}$) and $t_{1/2}$ of *Z*-isomers of compounds **1-9** at 298 K.

Compound	**1**	**2**	**3**	**4**	**5**	**6**	**7**	**8**	**9**
$\Delta H^{\ddagger}$ **(kJ/mol)**	92	92	93	98	101	96	96	92	79
$\Delta S^{\ddagger}$ **(J/mol*K^{-1})**	−41	−38	−47	−33	−22	−36	−37	−36	−50
$\Delta G^{\ddagger}$ **(kJ/mol)**	104	103	107	108	108	107	107	103	94
$t_{1/2}$ **(days)**	2.0	1.9	7.8	9.7	8.9	6.4	7.2	1.1	0.04

7. Thin film studies

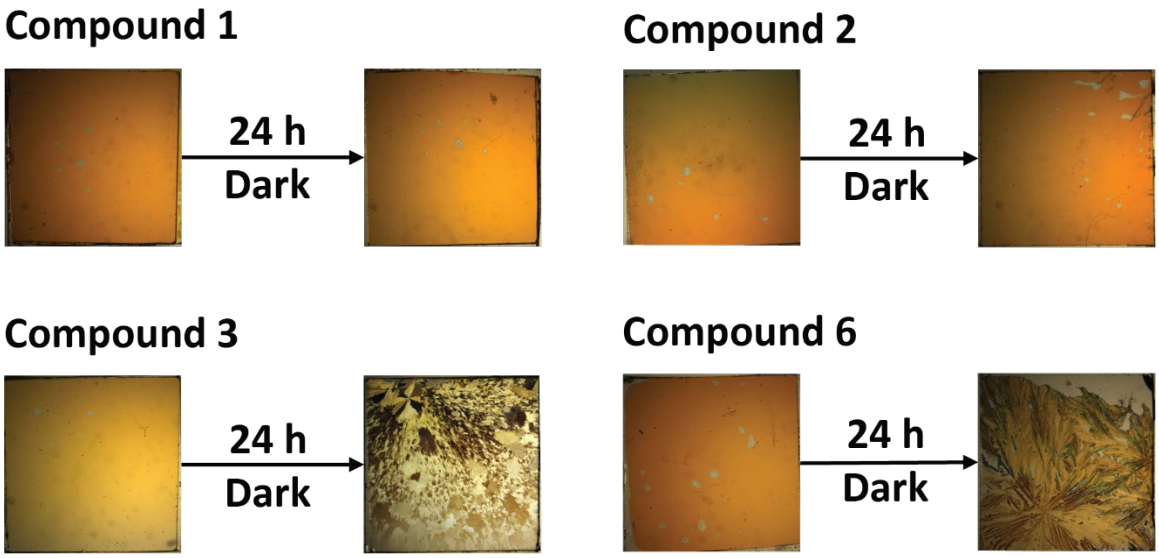

Fig. S6. Optical images demonstrating the stability of *Z*-rich liquid thin films of compounds **1**, **2**, **3**, and **6** in dark for 24 h.

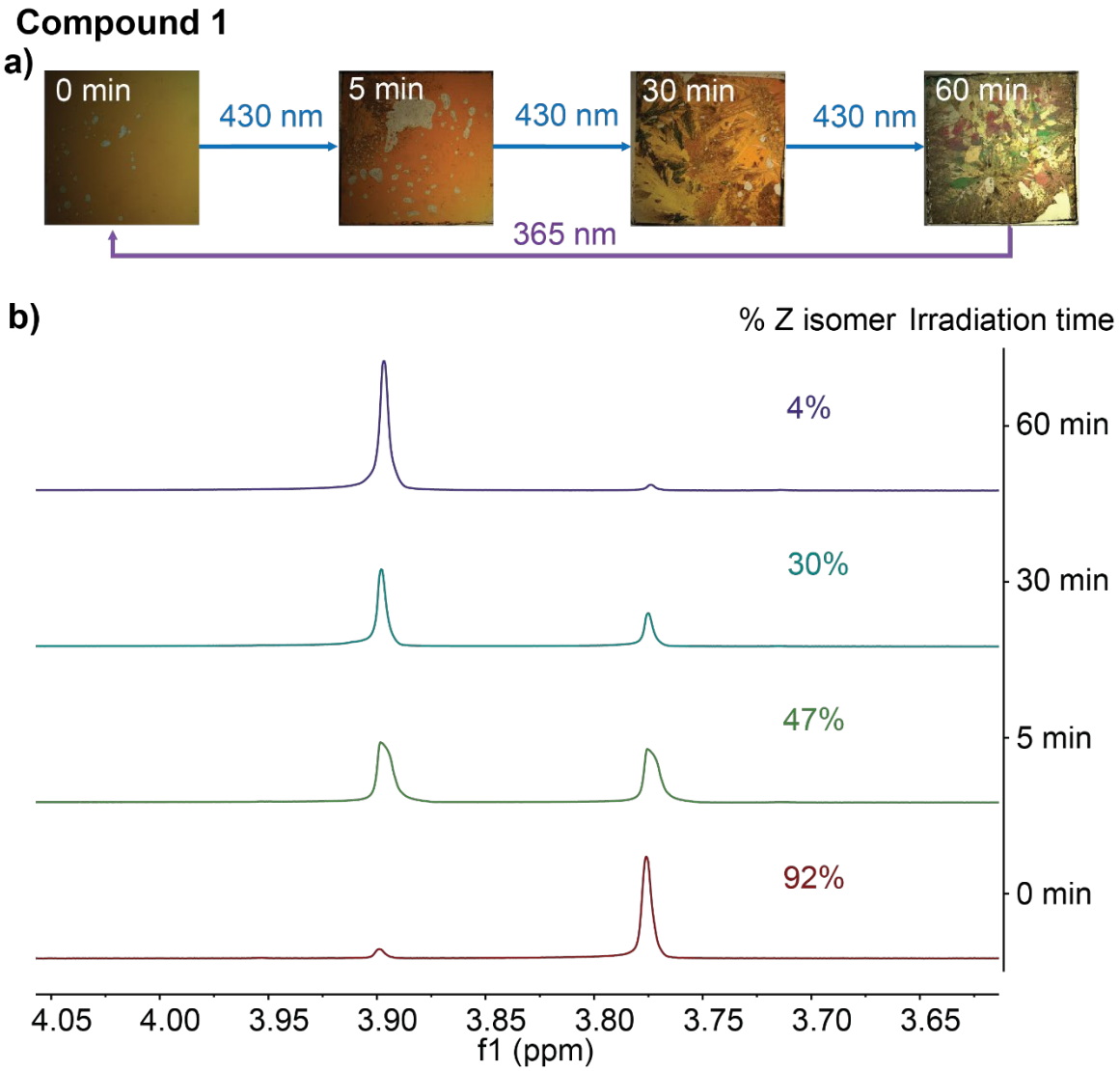

Fig. S7. a) Optical images demonstrating light-induced isomerization in a thin film of compound **1**. The images show the entire substrate (1.2 x 1.2 cm^2). The first image (0 min) shows a *Z*-rich film immediately after the irradiation by UV, and the following images illustrate the change of films with different 430 nm exposure time. b) The *Z* ratios of corresponding films were determined by ^{1}H NMR.

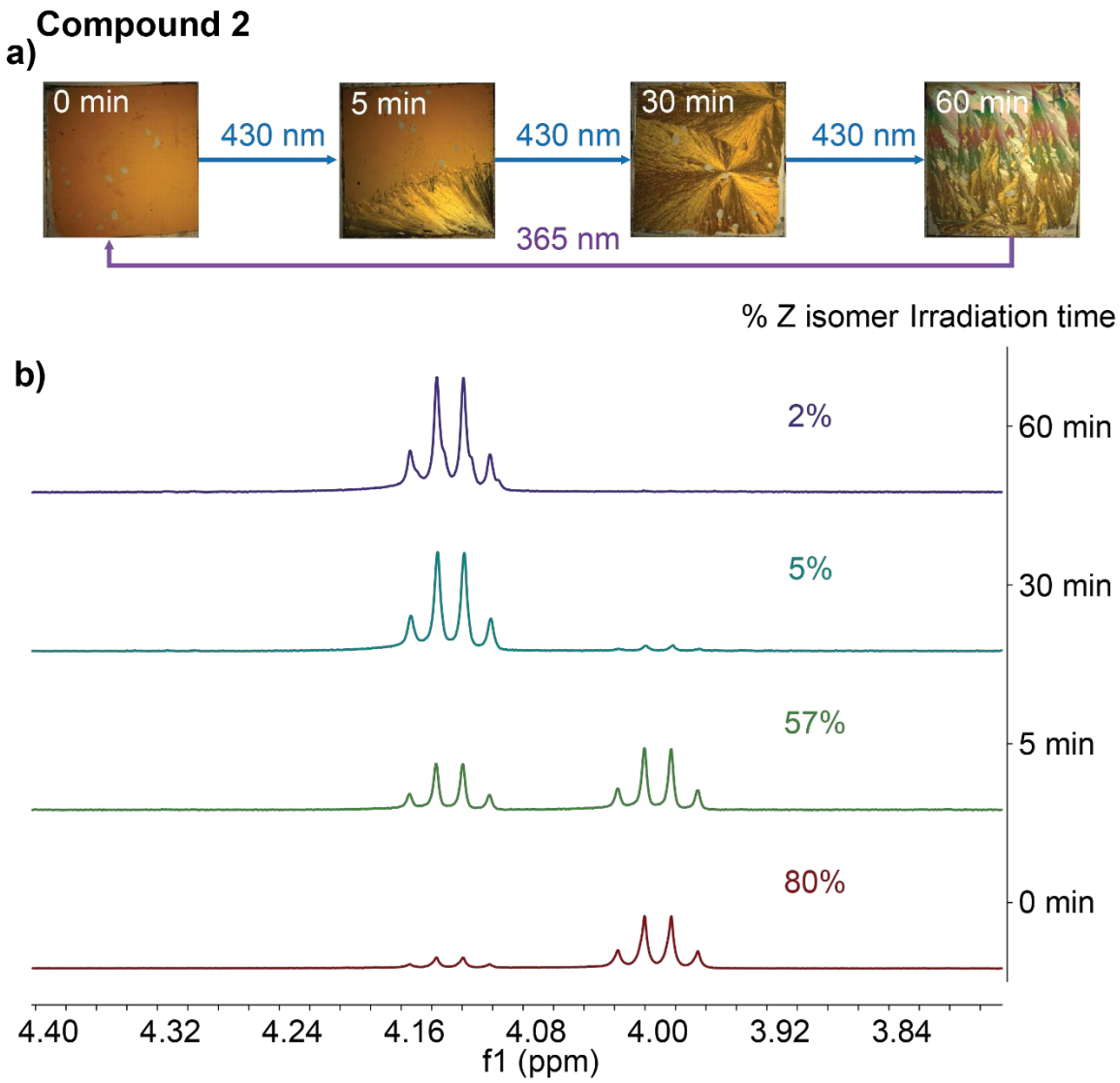

Fig. S8. a) Optical images demonstrating light-induced isomerization in a thin film of compound **2**. The images show the entire substrate (1.2 x 1.2 cm^2). The first image (0 min) shows a *Z*-rich film immediately after the UV irradiation, and the following images illustrate the change of films with different 430 nm exposure time. b) The *Z* ratios of corresponding films were determined by ^{1}H NMR.

8. Bulk sample isomerization

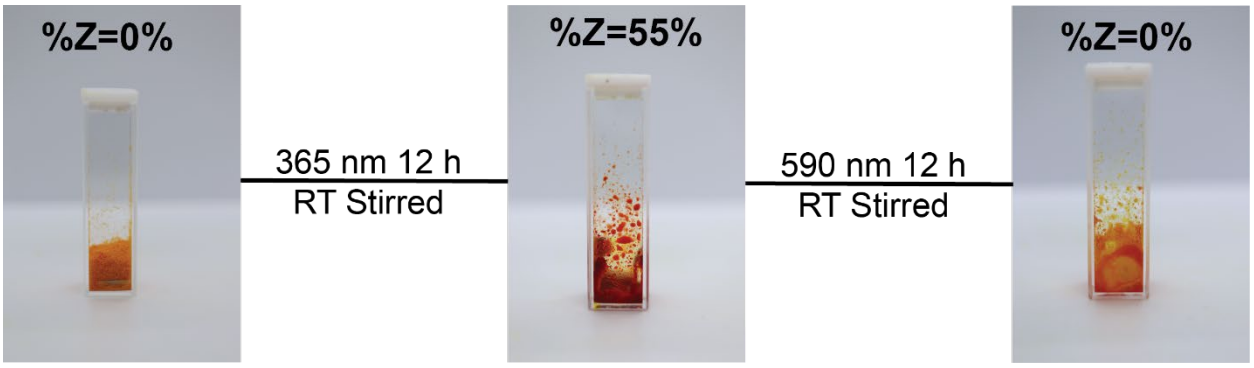

Fig. S9. The illustration of reversible phase transition and isomerization of compound **2** at 200 mg scale.

9. References

1 E. N. Cho, D. Zhitomirsky, G. G. D. Han, Y. Liu and J. C. Grossman, *ACS Appl. Mater. Interfaces*, 2017, **9**, 8679–8687.

2 V. A. Rassolov, M. A. Ratner, J. A. Pople, P. C. Redfern and L. A. Curtiss, *J. Comput. Chem.*, 2001, **22**, 976–984.

3 A. D. Becke, *J. Chem. Phys.*, 1993, **98**, 5648–5652.

4 H. Torii and M. Yoshida, *J. Comput. Chem.*, 2010, **31**, 107–116.

5 D. Hauchecorne, B. J. Van Der Veken, A. Moiana and W. A. Herrebout, *Chem. Phys.*, 2010, **374**, 30–36.

6 S. C. Cheng, K. J. Chen, Y. Suzaki, Y. Tsuchido, T. S. Kuo, K. Osakada and M. Horie, *J. Am. Chem. Soc.*, 2018, **140**, 90–93.

7 M. Volgraf, P. Gorostiza, S. Szobota, M. R. Helix, E. Y. Isacoff and D. Trauner, *J. Am. Chem. Soc.*, 2007, **129**, 260–261.

8 M. Schönberger and D. Trauner, *Angew. Chemie - Int. Ed.*, 2014, **53**, 3264–3267.

9 L. Wang, A. Ishida, Y. Hashidoko and M. Hashimoto, *Angew. Chemie - Int. Ed.*, 2017, **56**, 870–873.